Nature of polyamorphic transformations in H_2O under isothermal compression and decompression

Guoyin Shen,* Jesse S. Smith, and Curtis Kenney-Benson
High Pressure Collaborative Access Team, X-ray Science Division, Argonne National Laboratory, Argonne, Illinois 60439, USA

(Received 16 February 2019; published 31 July 2019)

We report polyamorphic transformations of H_2O under isothermal compression and decompression at 150 K, observed by *in situ* x-ray diffraction. Detailed structural information across the transformations among low-, high-, and very-high-density amorphs (LDA, HDA, and VHDA) reveals the mechanisms, the reversibility, and (dis)continuity of the transformations. During isothermal (de)compression, the polyamorphic transformations are characterized by a sharp and reversible LDA-VHDA transformation, with an HDA-like form (referred to as HDA′) appearing as an intermediate state. The LDA-VHDA transformation is found to occur in two steps: a discontinuous transition between LDA and the end member of HDA′ on the low-pressure side, followed by a continuous change within HDA′ involving structural reconfigurations and finally converging to VHDA. Both LDA and VHDA are found to be structurally stable showing mainly elastic behavior under (de)compression, while HDA′ is structurally unstable. Possible relations of these observations to low- and high-density liquids are discussed.

DOI: 10.1103/PhysRevMaterials.3.073404

I. INTRODUCTION

H_2O can exist in several amorphous forms (polyamorphism) at low temperatures. Understanding the relations among different polyamorphs is important for a coherent picture of the thermodynamic and transport properties of supercooled and glassy water and the liquid-liquid critical point [1–5]. At low temperatures, amorphous H_2O is generally categorized into three polyamorphs in terms of density, namely low-, high-, and very-high-density amorphs (LDA, HDA, VHDA) [3,4,6–8]. HDA can be produced by pressurizing hexagonal (I_h) or cubic ice (I_c) at 77 K to above 1 GPa [9], whereas LDA can be formed by rapidly supercooling water or by heating HDA at ambient pressure up to 125 K [8]. Between 125 and 140 K, the LDA-HDA transformation is reversible under isothermal compression and decompression, displaying a first-order-like transition with a hysteresis [8,10–12]. The pressure-induced HDA at 77 K is an unrelaxed glassy form (*u*HDA). By annealing at pressures below 0.5 GPa, a more relaxed form (so-called expanded HDA, *e*HDA) with a decrease in density is formed [13]. When *u*HDA is annealed at pressures above 1 GPa, a form with a density ∼9% higher than that of *u*HDA is formed, which is termed VHDA [6]. Recent experiments show that VHDA and *e*HDA are the most relaxed amorphs at high and intermediate pressures, respectively [14]. It remains a subject of debate whether HDA and VHDA experience a sharp transition upon isothermal (de)compression at low temperatures [14–17]. It has been pointed out that the nature of the (dis)continuity is possibly related to the rate of (de)compression [12].

At short-range scale, an increased occupancy of the interstitial molecules may account for the structural difference between LDA, HDA, and VHDA [18,19]. LDA is a tetrahedrally coordinated oxygen network with well-separated first and second coordination shells, similar to ice I_h, without any interstitial H_2O molecules in between the shells. On the other hand, there are two interstitial H_2O molecules in VHDA, accounting for 100% occupancy. *e*HDA seems to be in the middle and display one H_2O interstitial molecule at ambient pressure, i.e., 50% occupancy [18,19]. Thus at ambient pressure, the number of interstitial molecules increases from 0 to 1 and 2 for LDA to *e*HDA and VHDA, respectively. An arising question is whether there exist intermediate structures with intermediate interstitial numbers between 0–1 or 1–2, particularly at high pressures as VHDA and HDA become increasingly similar at increasing pressure [20,21]. At intermediate-range scale, simulations show that LDA may be viewed as a network dominated by six-membered rings, while HDA and VHDA include a significant fraction of longer member rings, associated with a network of substantial reconstruction [22]. Above 1 GPa, the VHDA network is dominated by eight- and nine-membered rings, which become structurally stable with further increasing pressure [23].

What is the nature of polyamorphic transformations among LDA, HDA, and VHDA? How many distinct amorphs in H_2O? Is HDA a third distinct state besides LDA and VHDA, as questioned by simulation studies [22–24]? Experimental studies of the relations among amorphous forms have been mainly based on isobaric annealing at ambient or modest pressures (<3 GPa). Because of the metastable nature, the isobaric annealing approach often involves irreversible processes such as relaxation, glass transition, and crystallization. Using isothermal (de)compression at various temperatures may be better suited for studying the phase relations among LDA, HDA, and VHDA, because it provides a density-driven approach for studying the polyamorphism that is categorized in terms of density. There are several studies using isothermal pathways [11,12,16,17,20,25,26]. While some studies show a small jump or a slope change in density across the

*gyshen@anl.gov

HDA-VHDA transformation [11,12,25], other studies using similar isothermal approaches do not support such density change, but indicate a smooth change in density in the similar pressure-temperature ranges [8,17,26]. The discrepancy may be understood by different kinetics, such as (de)compression rate [14]. Thus experiments at higher temperatures are desirable for suppressing the effect of kinetics. However, for bulk H_2O samples, it is reported that crystallization occurs under decompression of VHDA at temperatures above 140 K [25]. To suppress the crystal nucleation, emulsified ice samples consisting of small ice particles [16] have been adopted for isothermal experiments above 140 K. Recently, rapid (de)compression [27–29] has been implemented with *in situ* diffraction measurements for studying amorphous H_2O above 140 K under isothermal (de)compression. The results show that LDA (HDA or VHDA) can be formed from crystalline ice VIII (ice I_c) by rapid decompression (compression) [27,28]. Direct amorphous transformations between LDA and HDA (or VHDA) have been also observed under rapid compression or decompression [27,29]. In this paper, we present the *in situ* x-ray-diffraction study of amorphous forms under isothermal (de)compression 150 K, a temperature close to or even higher than the glass-transition temperatures of LDA, HDA, and VHDA [30,31]. Our studies are aimed at providing detailed insight into the structural changes across transformations among LDA, had, and VHDA, and their reversibility as well as the (dis)continuity of the transformations.

II. EXPERIMENTAL PROCEDURES

We used a double-sided membrane-controlled diamond-anvil cell (DAC) [32] for rate-controlled isothermal (de)compression experiments. Diamond anvils with a culet size of 500 μm diameter were used for pressure generation. The water sample (deionized ultrafiltered water from Fisher) was loaded in a preindented rhenium gasket with a chamber 150 μm in diameter and 50 μm thick. A few small ruby balls of $<5\,\mu$m diameter were loaded in the chamber together with a few micrometer-sized grains of gold powder for pressure measurements. The membrane DAC assembly was then loaded in a cryostat. *In situ* x-ray diffraction under isothermal (de)compression was carried out at the 16-ID-B HPCAT beamline at the Advanced Photon Source. Monochromatic x rays at 30.491 keV ($\lambda = 0.40663$ Å) were focused to a beam size of $\sim 3 \times 6\,\mu m^2$ (vertical $\times$ horizontal, full width at half maximum) with a photon flux of $\sim 8 \times 10^{11}$ photons/s at the sample position [33]. The use of the double-sided membrane system allowed us to perform multiple compression-decompression ramps on the same sample using a programmed routine. During isothermal compression-decompression stages we continuously collected x-ray diffraction using a Pilatus-1MF detector with a time interval of 0.050 s. Temperatures during the experiments were kept at 150 ± 0.2 K using a feedback loop [32].

III. RESULTS AND DISCUSSION

Two isothermal runs at 150 K (run I and run II) have been carried out. In run I, we compressed the sample to 3.3 GPa and then cooled down the cell in a cryostat. The pressure was found to have increased to 3.5 GPa at 150 K. X-ray diffraction indicated that the water sample transformed to ice VIII. We then rapidly decompressed the ice-VIII sample at a rate of -30 GPa/s. Consistent with our previous results [28], the rapid decompression resulted in a sharp change from ice VIII to an amorphous form [Fig. 1(a)] with the first sharp diffraction peak (FSDP) at ~ 1.71 Å^{-1}, indicating that the amorph is LDA [19]. We waited for 3 s and found that the LDA amorph remained over that period. After that, we compressed the LDA sample at a modest rate of ~ 0.8 GPa/s. At about 0.6(1) GPa, estimated from the Au(111) peak, LDA rapidly transformed to a different amorph with the FSDP at ~ 2.41 Å^{-1}, indicating that the transformed amorph is VHDA [19]. The LDA-VHDA transformation is sharp, but involves a detectable intermediate amorphous form with varying FSDP positions from 2.13 to 2.41 Å^{-1} [Fig. 1(b)]. Because the initial FSDP position at 2.13 Å^{-1} is very close to that of HDA at 0.5 GPa (~ 2.12 Å^{-1}) [34], the intermediate amorph is referred to as HDA′ here. Upon further compression, VHDA displayed mainly elastic compression as the FSDP position smoothly increases with pressure [Fig. 1(b)]. At ~ 1.5 GPa, ice VII starts to appear. Up to the highest pressure (2.9 GPa) of run I over a period of ~ 18 s, we observed the coexistence of VHDA and ice VII, even though the growth of ice VII was almost completed [Fig. 1(c)]. Similarly in run II (Fig. 2), we first compressed the sample to 3.4 GPa and then cooled down to 150 K. The starting H_2O form was also the ice-VIII phase at 3.6 GPa and 150 K. We rapidly decompressed the sample at a rate of -30 GPa/s and, as expected, found that ice VIII directly transformed to LDA close to ambient pressure [Fig. 1(a)]. After waiting for 2 s, we then compressed the LDA sample at a slow rate of 0.05 GPa/s and found the sharp transformation from LDA to VHDA at ~ 0.5 GPa, with a clear intermediate form (HDA′) during the transition [Fig. 2(b)]. About 7 s later at ~ 1 GPa, we started the third decompression ramp with a rate of -10 GPa/s on the transformed VHDA. At pressures close to ambient pressure, VHDA abruptly transformed to LDA, with a detectable intermediate form that is assigned to HDA′. The resultant LDA remained for at least 8 s at 150 K. The FSDP positions of polyamorphs in run I and run II are presented in Figs. 1(b) and 2(b), respectively. Overall, the characteristic feature of the polymorphic transformations under isothermal (de)compression at 150 K is the sharp and reversible transformations between LDA and VHDA, with an intermediate amorph (HDA′) across the transformations.

It is noted that the intermediate HDA′ appears to display a series of transient states in the HDA-family, with *e*HDA as end member on the low-pressure side and VHDA as end member on the high-pressure side, as indicated by its FSDP positions ([Figs. 1(b) and 2(b)]. Figures 1(d)–1(f) and 2(c) and 2(d) show the details of the diffraction patterns near the LDA-VHDA transformations for run I and run II, respectively. In run I, the compression of LDA in a time interval of 1.2 s right before the transition is shown in Fig. 1(d). Here LDA does not undergo clear structural changes, but displays a small shift in FSDP to higher Q values, suggesting a largely elastic compression of LDA corresponding to a pressure change of ~ 0.6 GPa. This elastic compression is followed by an abrupt transition from LDA to an end member of HDA′ on the

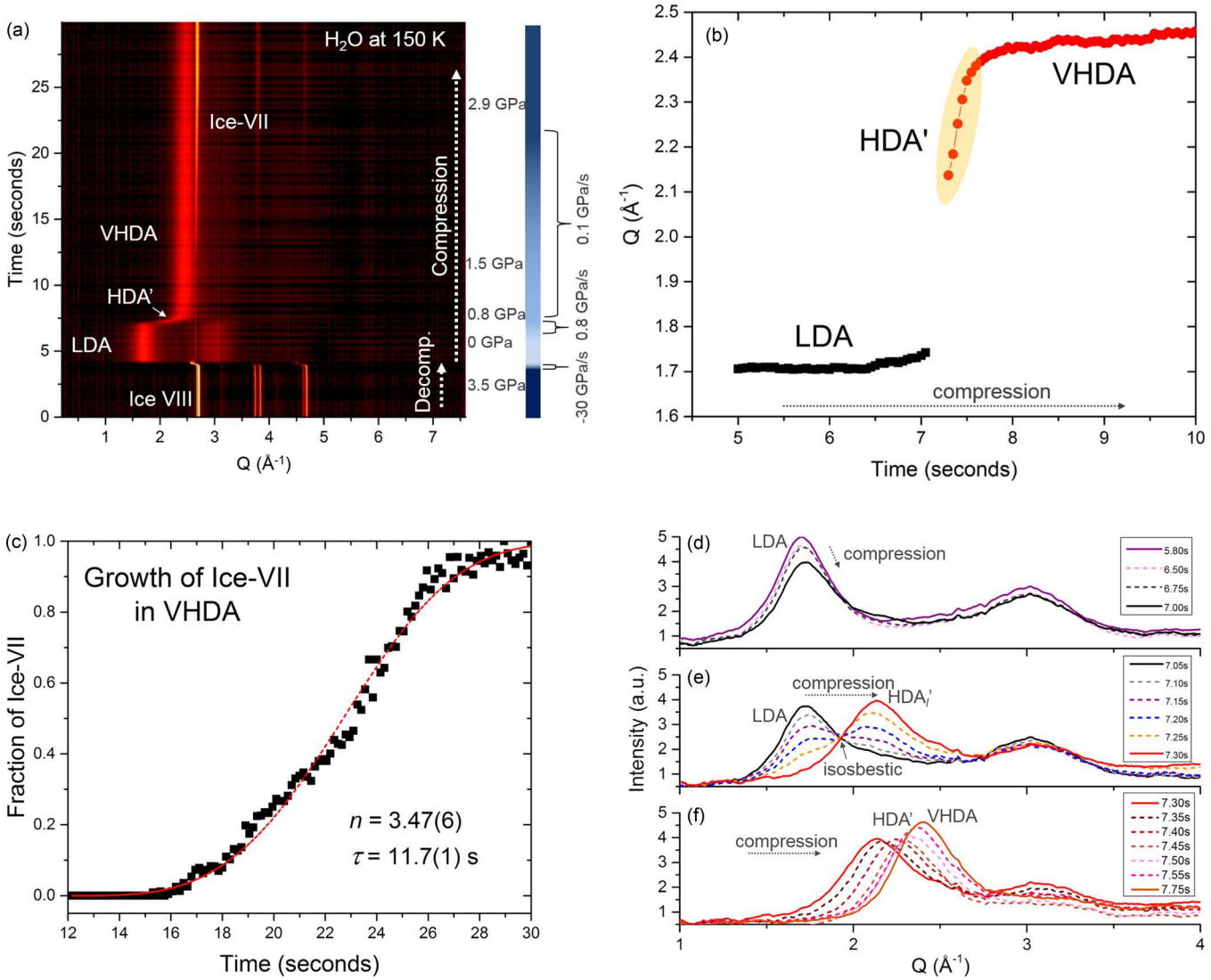

FIG. 1. Experimental data from run I. (a) Contour plot with x-ray-diffraction intensity in temperature scale displaying the changes of *in situ* diffraction for H_2O under isothermal (de)compression at 150 K. The starting material ice VIII is rapidly decompressed and transformed to LDA. Subsequent compression of LDA results in a relatively sharp transformation to VHDA, with an intermediate form HDA′. Upon further compression of VHDA, the crystallization of ice VII appears. (b) Positions of the first sharp diffraction peak are plotted against time. Position points are obtained using Gaussian peak fitting to diffraction patterns, with errors comparable to the symbol sizes. FSDP data display a discontinuous jump from LDA to HDA′$_l$, whereas the FSDP positions within HDA′ (highlighted) change rapidly, but continuously, and eventually converge into that of VHDA. **(c)** The growth of ice VII out from VHDA. The data points of the fraction of ice VII in black squares are obtained using the diffraction intensities of the (110) peak of ice VII. The fit to Avrami equation is plotted as the red dashed line, with the parameters shown in the figure. (d) *In situ* x-ray-diffraction patterns near the LDA-VHDA transformation, with time in seconds labeled in the figures. LDA patterns in 1.2 s right before the transformation, displaying a smooth shift of FSDP to higher Q. (e) Diffraction patterns across the LDA-HDA′$_l$ transformation in 0.25 s. An isosbestic point is obvious during the transformation. (f) Rapid and continuous shifts to higher Q corresponding to the highlighted area in (b).

low-pressure side (denoted as HDA′$_l$) in the next interval of 0.25 s [Fig. 1(e)]. An isosbestic point across the LDA-HDA′$_l$ transformation is clearly visible in Fig. 1(e), suggesting a coexistence of LDA and HDA′$_l$. The FSDP intensities of HDA′$_l$ continuously grow at the expense of LDA. A similar isosbestic point is also observed in run II in the compression pathway across the LDA-HDA′$_l$ transformation [Fig. 2(c)]. The observed coexistence of LDA and HDA′$_l$ is consistent with the interpretation of neutron data under isothermal compression at 130 K [34]. It is interesting to note that an isosbestic point was also observed across the *e*HDA-LDA transformation in annealing experiments at ambient pressure [35]. In the discontinuous LDA-HDA′$_l$ transition, the FSDP positions of HDA′$_l$ remain around 2.13 $Å^{-1}$, which is close to that of HDA at 0.5 GPa [34]. So, the coexistence of LDA and HDA′$_l$ strongly supports the view that the LDA-HDA′$_l$ transformation is first-order-like [5,7,11,35–37]. This transition is followed by a very different transition involving continuous structural changes within the intermediate HDA′ in the following 0.25 s. As shown in Fig. 1(f), under further

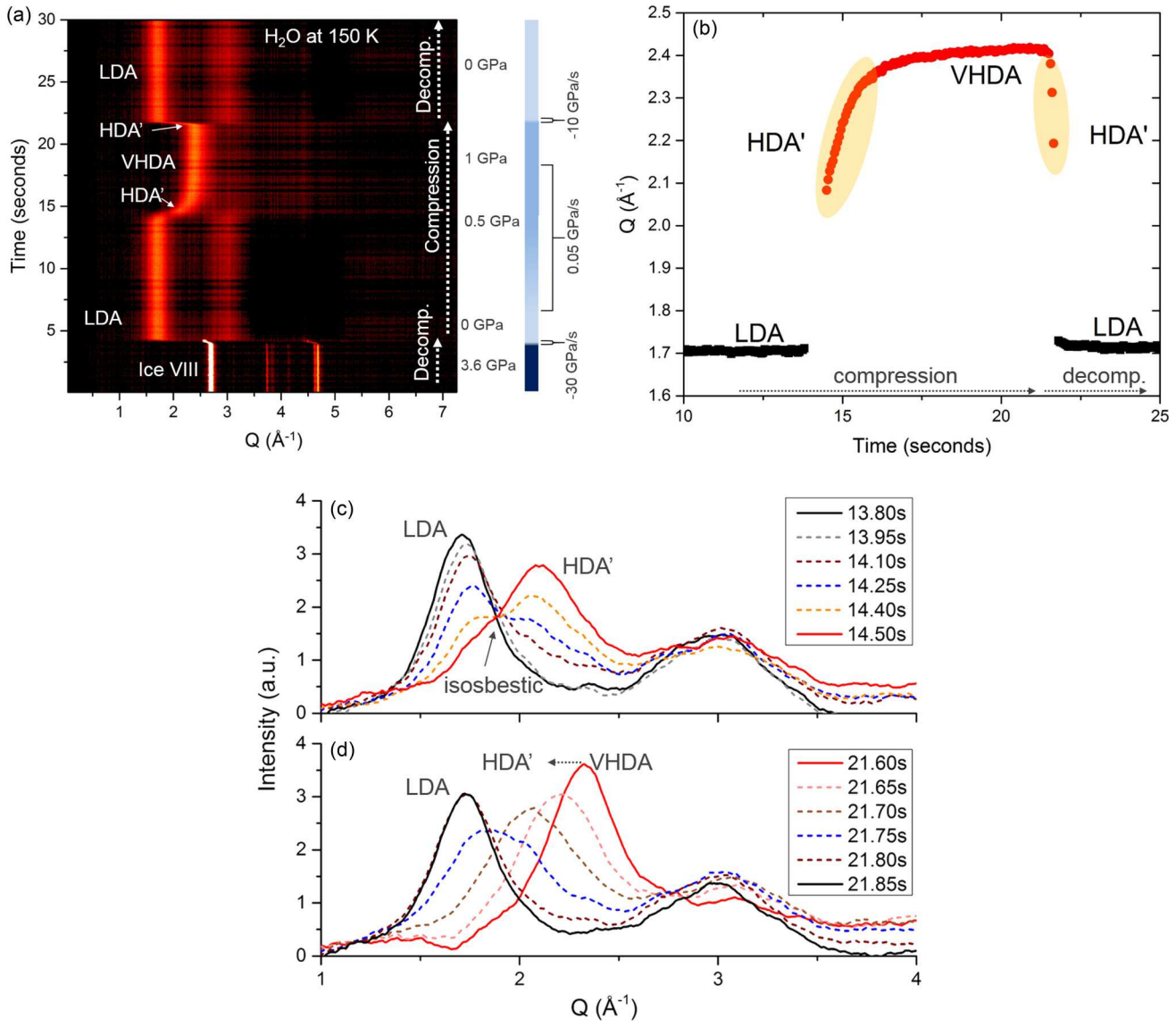

FIG. 2. Experimental data from run II. **(a)** Counter plot of x-ray-diffraction intensity for H_2O under isothermal (de)compression at 150 K. An additional decompression ramp is included in run II after the VHDA is formed by compressing LDA. These data show that the LDA-VHDA transformation in H_2O under isothermal (de)compression at 150 K is sharp and reversible. (b) Features in the first 22 s are similar to those in run I [Fig. 1(b)]. After that, VHDA is decompressed, with rapidly decreasing FSDP followed by an abrupt shift to that of LDA. **(c)** *In situ* x-ray-diffraction patterns near the LDA-VHDA transformations, with time in seconds labeled in the figure. Diffraction patterns across the LDA-HDA′ transformation in 0.7 seconds under compression, with a clear isosbestic point during the transformation, indicating a coexistence of LDA and HDA′. (d) X-ray-diffraction patterns under rapid decompression of VHDA, showing fast and continuous shifts to lower Q corresponding to the highlighted area on the right in (B). At the time of 21.75 s, the diffraction pattern (in dashed blue) displays a doublet corresponding to FSDPs of LDA and HDA′, respectively.

compression at the same compression rate (0.8 GPa/s) the FSDP of HDA′ continuously, and rapidly, shifts to higher Q until converging on the positions of the high-pressure side of HDA′ (i.e., VHDA) at 1–1.5 GPa. We obtained similar results from run II as shown in Fig. 2(b). It clearly shows that HDA′ is an intermediate form in the transformation from LDA to VHDA. Our diffraction data are qualitatively consistent with the results of slope changes in $d\rho/dP$ measured by piston displacement in isothermal studies [11,12,25]. Upon further compression in run I, VHDA becomes stabilized in structure, and displays a mainly elastic compression with its compressibility similar to that of ice VII (Fig. 3). In run II, when the VHDA at ∼1 GPa was further rapidly decompressed with a rate of −10 GPa/s [Fig. 2(d)], the FSDP rapidly shifts to lower Q toward to the positions of HDA′, and then abruptly changes to positions of LDA [Fig. 2(b)]. Because of the fast decompression rate, there are only a limited number of patterns collected across the VHDA-LDA transformation during decompression in a time interval of 0.25 s. However, it is noted that (1) the VHDA-LDA transformation is mediated by an amorphous form (HDA′) before forming LDA, and (2) at time of 21.75 s in Fig. 2(d), the diffraction pattern appears to have two peaks, resembling the coexistence of HDA′ and LDA. These findings show a reversible

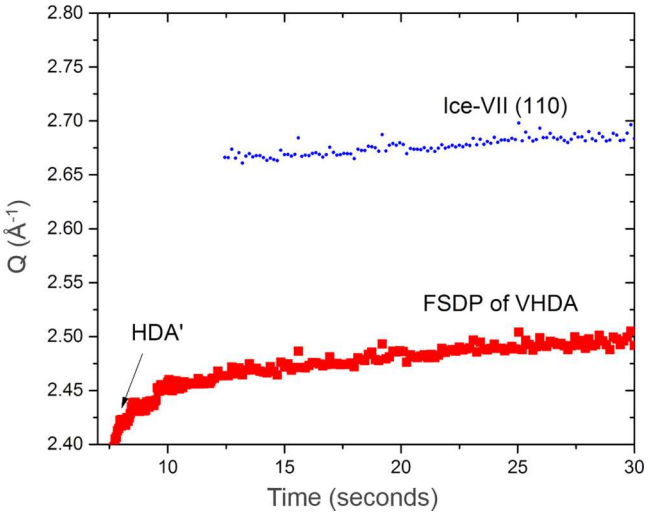

FIG. 3. Positions of the FSDP of VHDA are compared with the positions of the (110) diffraction peak of ice VII under isothermal compression. Compressibility of VHDA is similar to that of ice VII.

LDA-VHDA transformation, even including the reversibility of the intermediate HDA′. However, our temporal resolution of 0.05 s under decompression is insufficient to demonstrate a similar isosbestic point as displayed in LDA-to-HDA′$_l$ transformation [Figs. 1(d) and 2(c)] under compression. In principle, we could use a slower rate in decompression. But, because a slower decompression rate could cause crystallization of ice I_c [27,28], future experiments with higher temporal resolution are required to address a possible coexistence of HDA′ and LDA under isothermal decompression. It is noted that similar VHDA-LDA transformation was reported under rapid decompression above 140 K [27,29].

The highlighted areas in Figs. 1(b) and 2(b) show the FSDP positions of the intermediate HDA′. The large shift of the FSDP may represent continuous changes in ring sizes in the hydrogen-bonded network from dominant six-membered rings to longer member rings, associated with increasing occupancy of interstitial molecules between the first and the second coordination shells in HDA′ [18,19,22,23]. On the other hand, the clear discontinuity in FSDP between LDA and HDA′$_l$ (Fig. 2) suggests that there are no intermediate structures between LDA and HDA′$_l$. This is consistent with the findings of a large number of structural states between VHDA and *e*HDA, but not a single structural state between *e*HDA and LDA [25]. The existence of the isosbestic points shown in Figs. 1(d) and 2(c) indicates that LDA and HDA′$_l$ can coexist, perhaps in relatively large domains. These results may imply an atomistic picture at short-range scale: no intermediate structures with interstitial numbers between 0 and 1 can exist between the first and the second coordination shells, while continuous structural changes can occur with the number of interstitial molecules varying between 1 (50% occupancy) and 2 (100% occupancy) for HDA′, with the end member of 2 being the VHDA.

Since most previous diffraction studies are based on recovered samples at ambient pressure, *e*HDA has been viewed as a distinct metastable phase, e.g., Ref. [7]. However, our *in situ* x-ray-diffraction data suggest that *e*HDA may be only an end member of the intermediate HDA′ at 150 K. This result is generally consistent with the isothermal decompression studies at 140 K where VHDA was found to continuously evolve into HDA which in turn transforms discontinuously to LDA [11,25]. The fact that HDA′ is a transient phase may also be in agreement with the recent simulation studies where VHDA is found to be stable at positive pressures, whereas HDA is stable only at negative pressures [38].

The temperature in our experiments was kept at 150 ± 0.2 K, which is higher than the glass transition temperatures of LDA [35,39–41] and VHDA [30]. The process for forming LDA in our experiments is the same as that in a recent study [28] where a liquidlike form of LDA at 150 K is reported. So, it may be possible that the observed LDA here is also liquidlike. We subsequently compressed LDA and found that the LDA-VHDA transformation is followed by ice-VII crystallization nucleated from VHDA in run I [Fig. 1(a)]. The growth of ice VII displays a typical sigmoidal curve as a function of time [Fig. 1(c)]. The sigmoidal pattern is fitted using the Avrami equation:

$$f(t) = 1 - \exp[-(t/\tau)^n],$$

where τ is the characteristic time of the crystallization and n the dimensionality of the crystal growth, also referred to as the Avrami index. The obtained Avrami index ($n = 3.47$) is close to half integer, suggesting a diffusion-controlled growth of ice VII. The growth process may suggest that the observed VHDA could be liquidlike at 150 K, which is in general agreement with the liquidlike forms of HDA and VHDA at >140 K at high pressures [16,17,42]. If indeed the observed LDA and VHDA are liquidlike, our results on the LDA-VHDA transformations support the hypothesized liquid-liquid transition between low-density liquid (LDL) and high-density liquid (HDL) [1] and the view that VHDA is more closely related to HDL [24]. The transient nature of HDA′ implies that a low-lying HDA-VHDA critical point [15] may not be necessary. However, we consider that the current experimental evidence is still insufficient to conclude the liquidlike nature of the observed LDA and VHDA. More isothermal experiments with direct measurements on dynamics will provide experimental information for better understanding the LDL-HDL transition, the relations of VHDA-HDL and LDA-LDL, and the LDL-HDL critical point.

IV. SUMMARY

We have performed experiments on H_2O under an isothermal condition at 150 K by combining multiple compression and decompression pathways using a membrane-controlled DAC. An LDA form was synthesized by rapidly decompressing ice VIII. Under the subsequent compression, the LDA transformed to a VHDA. We find that LDA and VHDA are two distinct amorphous states under isothermal compression and decompression, and that the transformations between LDA and VHDA are repeatable, reversible, and sharp. An intermediate stage is noticeable in the transformation between LDA-VHDA, with a series of transient states (HDA′) ranging from *e*HDA as end member on the low-pressure side to VHDA as end member on the high-pressure side. The existence of intermediate HDA′ is consistent with the observations

in neutron-scattering experiments in transformations from VHDA to LDA, although neutron experiments were under annealing conditions at ambient pressure [43]. Both LDA and VHDA can be elastically compressed or decompressed, suggesting that they are structurally stable. The (de)compression of the intermediate HDA′, however, does not behave elastically, but involves continuous structural changes. So, we may view LDA and VHDA as two distinct metastable "phases," while HDA′ may be treated as doubly metastable with respect to LDA and VHDA. Our data do not support HDA to be a distinct third state. Nevertheless, this conclusion may be related to the temperature range in our study (150 K), because it is likely that the nature of HDA may be temperature dependent. Even though there is experimental evidence (including the growth mechanisms of ice I_c from LDA and ice VII from VHDA and the isothermal temperature being above the glass transition temperatures) suggesting the observed LDA and VHDA be liquidlike, more experiments on dynamics measurements are required for conclusively addressing the liquid nature of the amorphous forms.

ACKNOWLEDGMENTS

We thank Richard Ferry for technical support, and Yanbin Wang and Chris Benmore for useful discussions. G.S. acknowledges the support by the Department of Energy (DOE), Office of Basic Energy Science, Division of Materials Sciences and Engineering under Award No. DE-FG02-99ER45775, and the support by the National Science Foundation under Award No. EAR-1722495. High Pressure Collaborative Access Team operations are supported by DOE-NNSA's Office of Experimental Sciences. The Advanced Photon Source is a U.S. DOE Office of Science User Facility operated for the DOE Office of Science by Argonne National Laboratory under Contract No. DE-AC02-06CH11357.

[1] P. H. Poole, F. Sciortino, U. Essmann, and H. E. Stanley, Phase behaviour of metastable water, Nature (London) **360**, 324 (1992).

[2] J. A. Sellberg, C. Huang, T. A. McQueen, N. D. Loh, H. Laksmono, D. Schlesinger, R. G. Sierra, D. Nordlund, C. Y. Hampton, D. Starodub, D. P. DePonte, M. Beye, C. Chen, A. V. Martin, A. Barty, K. T. Wikfeldt, T. M. Weiss, C. Caronna, J. Feldkamp, L. B. Skinner, M. M. Seibert, M. Messerschmidt, G. J. Williams, S. Boutet, L. G. M. Pettersson, M. J. Bogan, and A. Nilsson, Ultrafast x-ray probing of water structure below the homogeneous ice nucleation temperature, Nature (London) **510**, 381 (2014).

[3] K. Amann-Winkel, R. Böhmer, F. Fujara, C. Gainaru, B. Geil, and T. Loerting, Colloquium: Water's controversial glass transitions, Rev. Mod. Phys. **88**, 011002 (2016).

[4] P. G. Debenedetti, Supercooled and glassy water, J. Phys.: Condens. Matter **15**, R1669 (2003).

[5] O. Mishima and H. E. Stanley, The relationship between liquid, supercooled and glassy water, Nature (London) **396**, 329 (1998).

[6] T. Loerting, C. Salzmann, I. Kohl, E. Mayer, and A. Hallbrucker, A second distinct structural "state" of high-density amorphous ice at 77 K and 1 bar, Phys. Chem. Chem. Phys. **3**, 5355 (2001).

[7] T. Loerting, K. Winkel, M. Seidl, M. Bauer, C. Mitterdorfer, P. H. Handle, C. G. Salzmann, E. Mayer, J. L. Finney, and D. T. Bowron, How many amorphous ices are there? Phys. Chem. Chem. Phys. **13**, 8783 (2011).

[8] O. Mishima, L. D. Calvert, and E. Whalley, An apparently first-order transition between two amorphous phases of ice induced by pressure, Nature (London) **314**, 76 (1985).

[9] O. Mishima, L. D. Calvert, and E. Whalley, 'Melting ice' I at 77 K and 10 kbar: A new method of making amorphous solids, Nature (London) **310**, 393 (1984).

[10] O. Mishima, Reversible first-order transition between two H_2O amorphs at ∼0.2 GPa and ∼135 K, J. Chem. Phys. **100**, 5910 (1994).

[11] K. Winkel, M. S. Elsaesser, E. Mayer, and T. Loerting, Water polyamorphism: Reversibility and (dis)continuity, J. Chem. Phys. **128**, 044510 (2008).

[12] T. Loerting, W. Schustereder, K. Winkel, C. G. Salzmann, I. Kohl, and E. Mayer, Amorphous Ice: Stepwise Formation of Very-High-Density Amorphous Ice from Low-Density Amorphous Ice at 125 K, Phys. Rev. Lett. **96**, 025702 (2006).

[13] R. J. Nelmes, J. S. Loveday, T. Strässle, C. L. Bull, M. Guthrie, G. Hamel, and S. Klotz, Annealed high-density amorphous ice under pressure, Nat. Phys. **2**, 414 (2006).

[14] P. H. Handle and T. Loerting, Experimental study of the polyamorphism of water. II. The isobaric transitions between HDA and VHDA at intermediate and high pressures, J. Chem. Phys. **148**, 124509 (2018).

[15] P. H. Handle and T. Loerting, Dynamics anomaly in high-density amorphous ice between 0.7 and 1.1 GPa, Phys. Rev. B **93**, 064204 (2016).

[16] O. Mishima, Relationship between melting and amorphization of ice, Nature (London) **384**, 546 (1996).

[17] Y. Suzuki and Y. Tominaga, Polarized Raman spectroscopic study of relaxed high density amorphous ices under pressure, J. Chem. Phys. **133**, 164508 (2010).

[18] J. L. Finney, D. T. Bowron, A. K. Soper, T. Loerting, E. Mayer, and A. Hallbrucker, Structure of a New Dense Amorphous ice, Phys. Rev. Lett. **89**, 205503 (2002).

[19] D. Mariedahl, F. Perakis, A. Späh, H. Pathak, K. H. Kim, G. Camisasca, D. Schlesinger, C. Benmore, L. G. M. Pettersson, A. Nilsson, and K. Amann-Winkel, X-ray scattering and O-O pair-distribution functions of amorphous ices, J. Phys. Chem. B **122**, 7616 (2018).

[20] S. Klotz, G. Hamel, J. S. Loveday, R. J. Nelmes, M. Guthrie, and A. K. Soper, Structure of High-Density Amorphous Ice Under Pressure, Phys. Rev. Lett. **89**, 285502 (2002).

[21] S. Klotz, T. Strässle, A. M. Saitta, G. Rousse, G. Hamel, R. J. Nelmes, J. S. Loveday, and M. Guthrie, In situ neutron diffraction studies of high density amorphous ice under pressure, J. Phys.: Condens. Matter **17**, S967 (2005).

[22] R. Martoňák, D. Donadio, and M. Parrinello, Polyamorphism of Ice at Low Temperatures from Constant-Pressure Simulations, Phys. Rev. Lett. **92**, 225702 (2004).

[23] R. Martoňák, D. Donadio, and M. Parrinello, Evolution of the structure of amorphous ice: From low-density amorphous through high-density amorphous to very high-density amorphous ice, J. Chem. Phys. **122**, 134501 (2005).

[24] N. Giovambattista, H. E. Stanley, and F. Sciortino, Relation between the High Density Phase and the Very-High Density Phase of Amorphous Solid Water, Phys. Rev. Lett. **94**, 107803 (2005).

[25] K. Winkel, M. Bauer, E. Mayer, M. Seidl, M. S. Elsaesser, and T. Loerting, Structural transitions in amorphous H_2O and D_2O: The effect of temperature, J. Phys.: Condens. Matter **20**, 494212 (2008).

[26] Y. Yoshimura, H.-k. Mao, and R. J. Hemley, Direct transformation of ice VII to low-density amorphous ice, Chem. Phys. Lett. **420**, 503 (2006).

[27] C. Lin, J. S. Smith, X. Liu, J. S. Tse, and W. Yang, Venture Into Water's no Man's Land: Structural Transformations of Solid H_2O Under Rapid Compression and Decompression, Phys. Rev. Lett. **121**, 225703 (2018).

[28] C. Lin, J. S. Smith, S. V. Sinogeikin, and G. Shen, Experimental evidence of low-density liquid water upon rapid decompression, Proc. Natl. Acad. Sci. USA **115**, 2010 (2018).

[29] G. Shen, J. S. Smith, C. Kenney-Benson, and R. A. Ferry, In situ x-ray diffraction study of polyamorphism in H_2O under isothermal compression and decompression, J. Chem. Phys. **150**, 244201 (2019).

[30] O. Andersson and A. Inaba, Dielectric properties of high-density amorphous ice under pressure, Phys. Rev. B **74**, 184201 (2006).

[31] T. Loerting, V. Fuentes-Landete, P. H. Handle, M. Seidl, K. Amann-Winkel, C. Gainaru, and R. Böhmer, The glass transition in high-density amorphous ice, J. Non·Cryst. Solids **407**, 423 (2015).

[32] S. V. Sinogeikin, J. S. Smith, E. Rod, C. Lin, C. Kenney-Benson, and G. Shen, Online remote control systems for static and dynamic compression and decompression using diamond anvil cells, Rev. Sci. Instrum. **86**, 072209 (2015).

[33] J. S. Smith, S. V. Sinogeikin, C. Lin, E. Rod, L. Bai, and G. Shen, Developments in time-resolved high pressure x-ray diffraction using rapid compression and decompression, Rev. Sci. Instrum. **86**, 072208 (2015).

[34] S. Klotz, T. Strässle, R. J. Nelmes, J. S. Loveday, G. Hamel, G. Rousse, B. Canny, J. C. Chervin, and A. M. Saitta, Nature of the Polyamorphic Transition in Ice Under Pressure, Phys. Rev. Lett. **94**, 025506 (2005).

[35] F. Perakis, K. Amann-Winkel, F. Lehmkühler, M. Sprung, D. Mariedahl, J. A. Sellberg, H. Pathak, A. Späh, F. Cavalca, D. Schlesinger, A. Ricci, A. Jain, B. Massani, F. Aubree, C. J. Benmore, T. Loerting, G. Grübel, L. G. M. Pettersson, and A. Nilsson, Diffusive dynamics during the high-to-low density transition in amorphous ice, Proc. Natl. Acad. Sci. USA **114**, 8193 (2017).

[36] K. Amann-Winkel, C. Gainaru, P. H. Handle, M. Seidl, H. Nelson, R. Böhmer, and T. Loerting, Water's second glass transition, Proc. Natl. Acad. Sci. USA **110**, 17720 (2013).

[37] P. H. Handle and T. Loerting, Experimental study of the polyamorphism of water. I. The isobaric transitions from amorphous ices to LDA at 4 MPa, J. Chem. Phys. **148**, 124508 (2018).

[38] R. V. Belosludov, K. V. Gets, O. S. Subbotin, R. K. Zhdanov, Y. Y. Bozhko, V. R. Belosludov, and J.-i. Kudoh, Modeling the polymorphic transformations in amorphous solid ice, J. Alloys Compd. **707**, 108 (2017).

[39] G. P. Johari, A. Hallbrucker, and E. Mayer, The glass–liquid transition of hyperquenched water, Nature (London) **330**, 552 (1987).

[40] A. Hallbrucker, E. Mayer, and G. P. Johari, Glass-liquid transition and the enthalpy of devitrification of annealed vapor-deposited amorphous solid water: A comparison with hyperquenched glassy water, J. Phys. Chem. **93**, 4986 (1989).

[41] M. S. Elsaesser, K. Winkel, E. Mayer, and T. Loerting, Reversibility and isotope effect of the calorimetric glass → liquid transition of low-density amorphous ice, Phys. Chem. Chem. Phys. **12**, 708 (2010).

[42] O. Andersson, Glass–liquid transition of water at high pressure, Proc. Natl. Acad. Sci. USA **108**, 11013 (2011).

[43] M. M. Koza, B. Geil, K. Winkel, C. Köhler, F. Czeschka, M. Scheuermann, H. Schober, and T. Hansen, Nature of Amorphous Polymorphism of Water, Phys. Rev. Lett. **94**, 125506 (2005).